Available online at www.sciencedirect.com

ScienceDirect

materialstoday: PROCEEDINGS

ELSEVIER

Materials Today: Proceedings 2 (2015) 4856 – 4865

Aluminium Two Thousand World Congress and International Conference on Extrusion and Benchmark ICEB 2015

Numerical assessment of the influence of process and geometric parameters on extrusion welds and die deformation after multiple-cycles

Tommaso Pinter[a,*], Barbara Reggiani[b], Lorenzo Donati[b], Luca Tomesani[b]

[a] *Almax-Mori S.r.l., Via Matteotti 13, Mori (TN) 38065, Italy*
[a] *University of Bologna, Viale Risorgimento 2, Bologna 40136, Italy*

Abstract

A comprehensive investigation on the correlation between die design and process parameters with extrusion welds (seam and charge) prediction and die deformation after multiple-cycles is presented. In particular, the influence of the number of legs (2,3 and 4) as well of some commonly adopted industrial best design practices in the extrusion of a round tube profile are examined by the ALE code HyperXtrude® for the AA6005A alloy. Then, for the same three designs, the die deformation after multiple-cycles is computed by applying a developed user sub-routine that account for the pressure and temperature maps and for the dwell-time that represents the time required to extrude each single billet. A sensitivity analysis on the influence of process parameters (ram speed, billet length and alloy) on the achieved die deformation after a fixed extruded amount is also performed.

Selection and Peer-review under responsibility of Conference Committee of Aluminium Two Thousand World Congress and International Conference on Extrusion and Benchmark ICEB 2015

Keywords: seam welds, charge welds, die deformation, multiple-cycles, extrusion, finite element

1. Introduction

Hot aluminum extrusion is a widespread process able to deal with complex profile geometries while ensuring high mechanical and aesthetical properties. However, since the flow conditions involved are product-specific, the

* Corresponding author. Tel.: +39-0464-916650; fax: +39-0464-910392
E-mail address: tommaso.pinter@almax-mori.it

Selection and Peer-review under responsibility of Conference Committee of Aluminium Two Thousand World Congress and International Conference on Extrusion and Benchmark ICEB 2015
doi:10.1016/j.matpr.2015.10.034

process optimization becomes a complex task that requires a comprehensive knowledge of the correlation between the input variables and the output parameters. In terms of input variables, it is well known that the die design is the most critical issue that directly influences the achievable production rate and product characteristics, both in terms of mechanical properties and dimensional tolerances.

Among the different profiles that can be manufactured, hollow profiles are marked by a higher level of complexity if compared to solid ones owing to the presence of a two-pieces (porthole) die involving a central mandrel required in order to define the internal shape of the profile and supported in the extrusion direction by two or more legs. The two main drawbacks of porthole dies are linked to their increased yielding (deflection) under the process loads due to a progressive accumulated plastic deformation, leading to the going out of the profiles tolerances [1], and to the formation of the so called longitudinal (seam) welds [2].

Concerning the mandrel deflection, the amount of the achieved accumulated deformation has been proved to be correlated with the specific service conditions acting in the creep-fatigue regime [3]. Fatigue manifests since each extruded billet represents a loading cycle for the die. In addition, accounting for the high process temperatures and for the non-negligible cycle times (dwell-time), also the creep phenomenon has to be accounted for in the die life prediction. The synergic effect of creep and fatigue emerges since the quote of plastic deformation accumulated in the same direction cycle by cycle under positive mean stress has to be added to that stored during each cycle time at constant load and high temperature for the creep effect. In previous works [4], the authors presented a novel theoretical model capable of deal with such type of predictions accounting for the pressure and temperature maps acting on the die and for the specific process dwell-time defined by the selected values of the ram speed and of the billet length. Even if a number of papers in literature report the effect of parameters like temperature and dwell-time on deformation under creep-fatigue regime [5], no previous studies show the effects on deformation on real industrial extrusion dies. In addition, a comprehensive evaluation of potential factors influencing the time-dependent deformation was not previously carried out.

The second shortcoming of hollow profiles, the seam welds, are formed due to the material splits around the legs in the extrusion direction that re-joints in the welding chamber before the bearing exit. The process conditions, such as the ram speed, the billet preheating temperature and the die geometry have been proved to strongly affect the welding state which, in turn, affect the production rate and can determine an earlier onset of defects [2,6]. Failure of hollow extruded products mostly occurs along one of seam weld lines when the products are subjected to severe internal pressure or expansion during their service life, thus representing the weakest points of the profile. However, if a systematic process and die design is performed thus ensuring the proper welding conditions, then seam welds can exhibit the same mechanical properties of the base material [7].

Together with the seam welds, the extrusion process involves a second type of welds generated between two consecutive billets and known as charge welds. The charge welds formation is a common phenomenon to both hollow and solid profiles and have been proved to strongly depend on the die geometry [8] while le influence of the billet material, ram speed and billet preheating temperature is uncertain [9]. It happens since at the end of a process stroke, the die remains completely filled by the old billet material so that when a new billet is loaded into the press, the old and new billets start to interact and a long transition zone is produced in the profile extruded after the stop mark. However, unlike seam, the charge welds are usually contaminated by oxides, dust, or lubricant so that the profile length affected by the charge weld must be discarded due to its inferior mechanical properties. As shown in [8], in order to effectively remove all the critical parts, two parameters are of critical importance: the position of the transition zone on the profile with respect to the stop mark and its extent.

Since the last years, in the extrusion context, finite element (FE) codes are becoming the most important tools for process and product optimization. The current state-of-the-art of numerical simulations applied to the extrusion process has been exploited by an extrusion benchmark conference in several past editions [10,11]. As a result, a generally significant increase of codes accuracy was found in the prediction of process load, material flow, pressure and temperature maps. By means of the numerical simulations, process parameters and die designs can now be optimized in order to enhance the product properties and, more in general, to increase productivity at a relatively low cost.

The objective of this study is to perform a comprehensive numerical investigation on the correlation between die design and process parameters with extrusion seam and charge welds prediction and die deformation after multiple-cycles. In particular, the influence of the number of legs (2,3 and 4) as well of some commonly adopted industrial

best design practices in the extrusion of a round tube profile of 51.5 mm as outer diameter and 2 mm wall thickness is examined. The seam welds quality is evaluated by inspecting the pressure, temperature and the velocity field in the welding chamber as predicted by the ALE code HyperXtrude® [12] for the AA6005A alloy. The effect of a different number of legs on the charge welds evolution is then evaluated by means of the same FE code in terms of percentage of new material over the stop mark distance with the aim to quantitatively assess the influence on the material to scrap. Then, for the same three designs, the die deformation after multiple-cycles is computed by applying, in a structural FE code, a developed user sub-routine that account for the pressure and temperature maps acting on the die in relation of the selected process setting. Moreover, the dwell-time is accounted for representing the time required to extrude each single billet. A sensitivity analysis on the influence of process parameters (ram speed, billet length and extruded alloy) on the achieved die deformation after a fixed extruded amount is also performed.

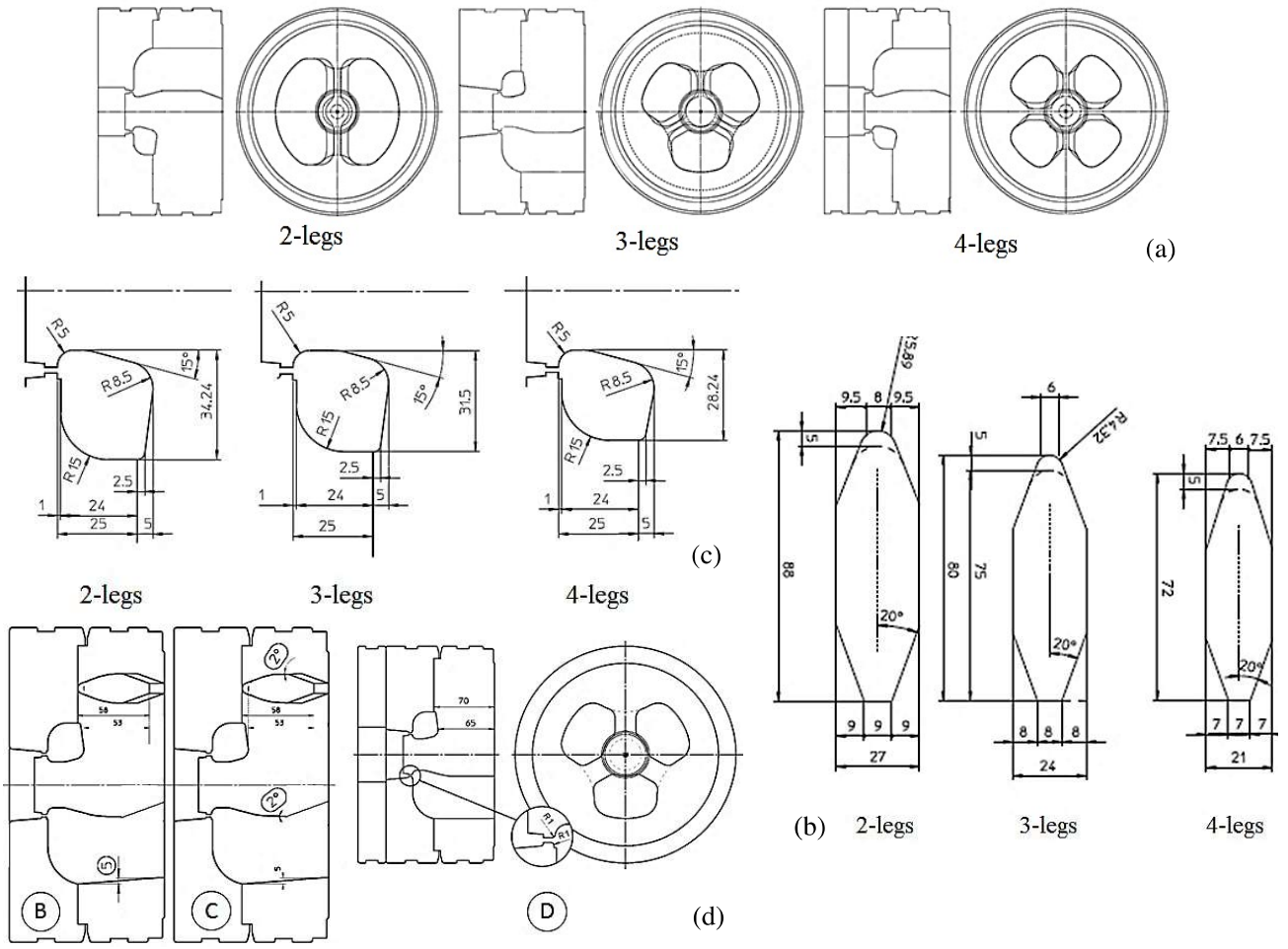

Fig. 1. The investigated die design modifications; (a) variations of the legs number and the detailed design of the legs (b) and of the welding chambers (c); the additional geometric variations: B) 5mm undercut on ports (divergent ports), C) 2° relief on mandrel and legs (divergent ports), D) radius of 1 mm on the bearings.

Table 1: Geometrical dimensions of welding chambers, legs and ports for the different die-legs configurations

Die geometry	Welding chamber			Legs			Ports	
	Width [mm]	Height [mm]	Area [mm^2]	Width [mm]	Height [mm]	Length [mm]	Total area [mm^2]	Width [mm]
2-legs	34.24	30	852.13	27	88	34.24	13184	49.5
3-legs	31.50	30	801.48	24	80	31.50	9578	49.5
4-legs	28.24	30	686.03	21	72	28.24	10286	49.5

2. The evaluated porthole die designs

In Fig. 1 are reported the investigated die modifications used to manufacture the round tube profile with an extrusion ratio of 110. As can be seen in Fig. 1a, the number of legs ranging from 2 to 4 is accounted for as main geometric parameter. As recommended by the dies manufacturers best practices, in a die the sum of the legs' cross sections, called resistant section, should not be smaller than the not-supported impact area (surface of the legs impacted by the aluminum flow, internal to the weld chamber perimeter). The dies used for the FE analyses are designed in a way that the resistant section is around 10% bigger than the impact area. Regarding the shape of the welding chamber, this is coming from internal best-practices. Considering a precise legs width, one determines the weld chamber width and, as a consequence, the shape of the weld chamber. Detailed designs and dimensions of the legs and of the welding chambers are reported in Fig. 1b,c and Tab. 1. For each legs configuration, additional geometric variations are investigated (Fig. 1d) defined according to a previous analyses performed by authors [13]. In the following, the “A” type with straight ports represents the base design for the different die-legs configurations with a chamfer of 20° on the legs.

3. Numerical DOEs and procedures

3.1. Seam welds quality

In order to investigate the effect of the selected die designs on the seam welds quality, steady-state simulations of the process were performed by means of the FE code Altair HyperXtrude® (HX) for each geometric configuration (12 simulations). Initially, only the billet was included in the models in the regime configuration (die already filled, profile extruded) (Fig. 12a). Special care was given to the preparation of the FE models in order to reduce at maximum the influence of the workpiece model architecture on the numerical results. In particular, an identical size of the tetra-elements was adopted for every model in the various workpiece sections (Fig. 2a,b).

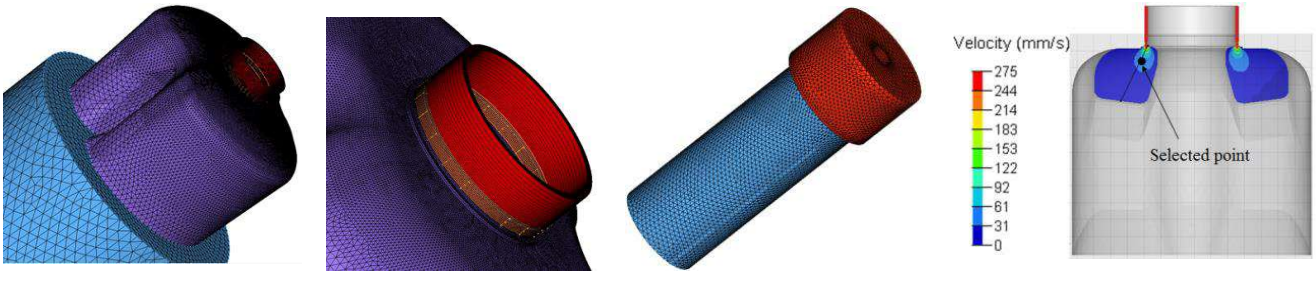

(a) (b) (c) (d)

Fig. 2. (a, b) The generated FE model of the sole billet and (c) with coupled die. (d) The point selected for the pressure and temperature monitoring used to evaluate the seam weld quality.

The aluminum (AA6005) was modelled as a non-Newtonian fluid by means of the Hansel-Spittel equation [14] whose constants were experimentally determined [15]. The temperatures of the billet, die and container were fixed

to 470°C, 500°C and 430°C respectively while the ram speed was set equal to 3 mm/s. The billet diameter and length were 210 mm and 500 mm. A sticking condition was imposed at the billet-tools interfaces except in the bearing regions where the viscoplastic model with a friction factor m=0.3 was used [8]. A convective coefficient of 1,500 W/m2°C was set between the billet and the container while 3,000 W/m2°C elsewhere. A second set of steady-state simulations was performed for the sole "A" configurations by including the die in the FE model (Fig. 2c) with the twofold aim of evaluating the effect of a coupled simulation on the process parameters influencing the seam welds strength and to extrapolate the temperature and pressure maps acting on the die to be applied for the computation of the multi-cycles deformation.

Results of the simulations are presented in terms of pressure and temperature in the welding chamber in a selected point far from the dead zones ($V < 10\% \cdot V_{max}$) (Fig. 2d for the 2-legs configuration). Indeed, according to [16], a seam weld quality index need to weight the ratio of pressure to effective stress according to the residence time, thus reducing the contribute of the low velocity areas. For this reason, the extension of the dead metal zone in the welding chamber is qualitatively monitored. The flow stress in the same point is also extrapolated and the P/σ index (P representing the contact pressure, σ the effective stress) computed. The peak pressures and temperatures inside the dies is monitored in order to amplify the potential differences, as well as the peak process load and profile temperature at 22 mm far from the die exit.

Since die design has a direct impact not only on the seam welds quality but also on the flow balance, the relative exit speed difference (r.e.s.d.) is computed as the percentage ratio of the difference between the peak and the average velocity over the average velocity in a profile section immediately after the bearing exit.

3.2. Charge welds evolution

The evolution of the charge welds was investigated only for the three "A" configurations at variable number of legs. Indeed, the "B", "C" and "D" designs produced only negligible variations of the ports volume and, in general, of the die geometry thus not significantly affecting the charge welds extension. The weld length calculation was performed by means of a transient analysis with moving boundaries in HX. In this type of problem, the boundary conditions for the flow and heat transfer equations are treated as time-dependent and the position of the billet–ram and of the billet–container interfaces are tracked during the simulation time. The mesh in the profile, bearing, porthole, and welding chamber remain fixed, but in the billet region, the elements scale down linearly in the extrusion direction at each time step. Validation of the HX code in the prediction of the charge welds length is reported in [8]. Results are presented in terms of extent, onset, and evolution behavior of the charge welds over the distance from the stop mark, i.e. the permanent shape marker on the profile indicating the end of a billet stroke. Die stress analysis and multi-cycles die deformation The permanent deformation of the three "A" die configurations made of H11 tool steel after multiple extruded billets was computed by means of a purposely developed analytical model presented in detail in [4] and implemented in an FE code dedicated to structural analyses with a sub-routine. The model accounts for the pressure and temperature maps acting on the die in relation of the selected process setting ad for the specific dwell-time, that is the time required to extrude each single billet. The pressure and temperature maps were extracted by the coupled steady state simulations previously performed and then exported to the structural code. The user sub-routine was modified with respect to what reported in [4] in order to group the temperature levels avoiding to exceed the number of admissible material models in the code. A comparison of the structural code predictions at the first static load by setting an elasto-plastic behavior of the die [4] was made with the results of the OptiStruct code [12] used to simulate the die with an elastic material model. Data are compared in terms of peak mandrel deflection in the extrusion direction and of peak equivalent stress in the die. A sensitivity analysis on the influence of process parameters on the achieved die deformation after a fixed extruded amount (5 tons) is also performed. In particular, the effect of an increased ram speed of 25% (3.75 mm/s), billet length of 50% (750 mm) and of an harder alloy (AA7020) are investigated and results discussed in terms of evolution of the permanent mandrel deflection over the amount of extruded material.

4. Results and Discussion

In Tab. 2 are presented the overall achieved results of the performed uncoupled simulations (no die in the FE model) for the different geometric configurations of die and legs.

An increased, even if small, load is observed moving from the 2-legs to the 4-legs for the "A" design (straight ports). This can be related to the increased friction due to the higher overall legs surface (Tab.1) for the 3 and 4-legs dies if compared to the 2-legs solution marked by higher legs height but in reduced number. The trend for the divergent ports "B" and "C" designs for the 2,3 and 4-legs indeed seems to make almost negligible the effect of the friction and to amplify the invers correlation with the ports area (Tab.1). This can be ascribable to the increased deformation throughout the ports if small ports instead of big ports are used.

Significantly marked is instead the effect of the radius of 1 mm on the bearings ("D") that reduced of an average 4% the peak extrusion load if compared to the "A" design due to the capacity of produce an even distribution of strain near the die exit.

Peak differences of 1% are shown in terms of profile exit temperature for the investigated die geometric configurations, with the maximum deviation for the "D" configuration.

The flow unbalance, evaluated by means of the relative exit speed difference (r.e.s.d.), shows a lower sensibility (lower values) to geometric variations for the 2-legs configuration. Even if a general trend is difficult to trace, by averaging the achieved results for the different designs ("A", "B", "C" and "D") it can be seen that a progressive increased unbalance is obtained for the 2, 3 and 4-legs related to corresponding increased number of obstacles, the legs, to the material flow in the extrusion direction. An increased extension of the dead metal zone (DMZ) is reported for the 2-legs solution.

Table 2. Results of the performed FE uncoupled (without die) steady-state simulations (HX) and of the dies stress analyses (Optistruct)

	Load [MN]	Pressure [MPa]		Flow stress	P/σ	Temperature [°C]			Velocity	DMZ (velocity mm/s)
		WC	max	σ [MPa]		WC	profile	max	r.e.s.d	
2-legs										
A	17.87	183	361	25	7.32	534	586	591	0.31	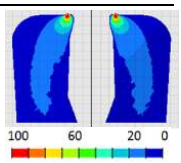
B	17.96	185	363	25	7.40	533	586	591	0.32	
C	18.10	189	366	25	7.56	533	586	591	0.27	
D	17.27	177	350	24	7.38	532	579	583	0.16	
									Avg. 0.27	
3-legs										
A	18.21	185	364	24	7.71	530	587	593	0.08	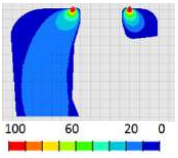
B	18.48	190	369	24	7.92	531	586	592	1.28	
C	18.49	191	368	24	7.96	530	586	592	0.25	
D	17.39	175	346	24	7.29	529	580	583	0.21	
									Avg. 0.45	
4-legs										
A	18.45	189	368	24	7.88	535	587	592	0.07	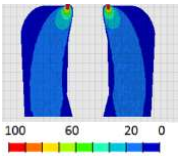
B	18.05	182	358	24	7.58	535	587	592	0.68	
C	18.04	186	361	24	7.75	535	586	593	2.40	
D	17.39	177	347	24	7.38	535	585	584	2.28	
									Avg. 1.36	

4.1. Seam welds quality

If the effect of the single geometric parameters is analyzed in terms of welding chamber pressure for the "A" configurations, it can be stated that a greater welding chamber width is detrimental for pressure [17] while greater ports area is beneficial leading to higher pressure in the welding chamber [2]. Moving from the 2-legs to the 4-legs solution, the welding chamber width is decreased (Fig. 1c) and the ports area has no trend. Observing the increased value of the welding chamber pressure as numerically predicted for the various legs solutions, it can be concluded that the most affecting parameters for the pressure is the welding chamber width. The convergent solutions ("B" and

"C"), as well as the "D" design, produce on the welding pressure the same effect previously overserved for the extrusion load.

In the same point used to track the welding pressure (Fig. 2d) also the flow stress is evaluated and used to compute the welding criteria P/σ. In each case an high value is obtained that ensure sound seam welds.

A peak variation of 1.1% in terms of welding chamber temperature is achieved between the 4-legs solution and the "D" design of the 3-leg solution, a scatter that can be considered negligible for the outcome weld quality.

No significant differences are found for the temperature and pressure in the welding chamber as predicted by the steady state simulations without (uncoupled) and with the die (coupled) included in the FE model.

4.2. Charge welds evolution

In Fig. 3 is reported the charge weld evolution, in terms of percentage of the new material, over the stop mark distance for the three configurations, 2, 3 and 4-legs (Fig. 3a,b), as computed by means of HX. The onset and exhausting points of the charge weld length for each solution are reported in Fig. 3c for a 100% of replacement of the old billet with the new billet material and for a value of replacement of 99%. As expected, the 2-legs configuration shows delayed onset and exhausting point with respect to the 3 and 4-legs. This is owing to higher volume ports of the 2-legs configuration together with the increased extension of the dead metal zones (Tab. 2). No significant difference emerge between the 3 and 4-legs solutions probably related to a balancing of the extended friction surfaces (increase the charge weld length) with the reduced ports volume (decrease the charge weld length) for the 4-legs if compared to the 3-legs die. The total weld length for the 2-legs is 10,570 mm if the 100% of replacement is considered (Fig. 3c) while it is reduced to 5,230 mm considering a 99% of replacement. For the 3-legs the corresponding computed weld lengths are 7,450 mm (100%) and 3,970 mm (99%) with a negligible difference with the 4-legs. These values have to be compared with the common industrial practice to scrap 3,000 mm after the stop mark for extrusion ratios exceeding 40 [8] thus highlighting the requirement to perform accurate investigations in order to effectively remove all the critical profile length.

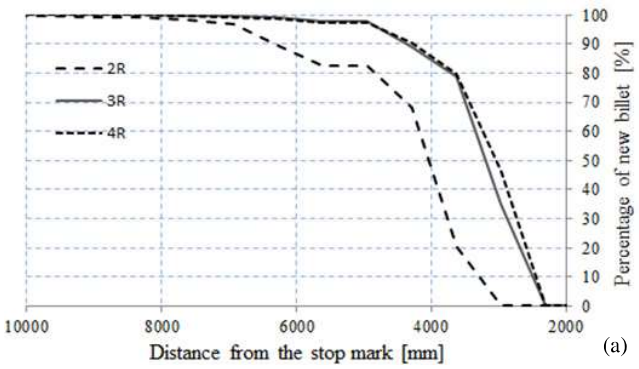

(a)

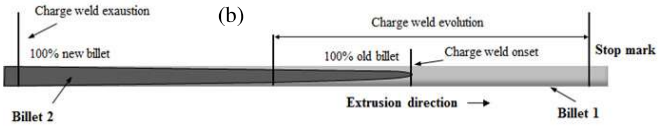

Die	Start-stop distance from the stop mark [mm]	
	100%	99%
2-legs	2970 – 13540	2970 – 8200
3-legs	2300 – 9579	2300 - 6270
4-legs	2300 – 9581	2300 - 6280

(c)

Fig.3. (a) Evolution of the charge weld over the stop mark distance; (b) schematic explanation of the charge weld formation and nomenclature; (c) onset and exhausting points of the charge welds for the 100% and 99% of replacement of the old billet with the one.

4.3. Die stress analysis and multi-cycles die deformation

In Tab. 3 are reported the design of experiment (DOE) of the simulations performed in the structural code to predict the multi-cycle die deformation. The dwell-time resulting from the set ram speed and billet length is also reported. For each design (raw), the minimum and maximum values of the temperature and pressure maps as predicted by the process simulation with coupled die are shown. Additionally, a comparison of the die stress analysis output (static load) for the "A" base design in terms of peak von Mises stress and deflection (UZ) under load in the extrusion direction of the die is presented between what predicted by the structural code at the first load cycle and the numerical estimations of Optistruct. In the former case, an elasto-plastic material model was used while in the latter a linear elastic behavior was set. As can be seen, the hypothesis of an elastic behavior leads to an overestimation of the 44% and 35% of the peak stress in the die and of an underestimation of 2% and 18% of the die deflection for the 2 and 3-legs solutions if compared to more realistic predictions with an elasto-plastic model. This clearly indicates the requirement to select accurate material models in order to achieve meaningful results. No significant differences are found between the 3 and 4-legs configurations. Concerning the multi-cycles deformation of the die, results are presented in Fig. 4 in terms of peak mandrel deflection under load over the total extruded tons, these calculated accounting for the number (ratio of the simulation time on the dwell-time) and length of the processed billets. The 2-legs solution shows the most reduced support effect to the mandrel deflection with the highest level of deformation in each tested conditions if compared to the 3 and 4-legs configurations that appear progressively less susceptible to process parameters variation (reduced scatter among the curves).

The extrusion of an harder alloy (AA7020) than the AA6005 represents the most critical conditions for all the die configurations; a peak difference of 25%, 14% and 10% between the base design deflection with the AA6005 and that with the AA7020 alloy at 5 extruded tons is predicted for the 2, 3 and 4-legs respectively. In the 2-legs solution, the increased dwell-time for the 50% longer billet involves the same effect of an increased 25% of ram speed. This can be explained by the increased temperature in the die (598 °C) generated by the higher ram speed that produces that same detrimental effect of an increased dwell-time in terms of accumulated deformation.

Table 3. Numerical DOE and results of the performed simulations for the die stress analysis and the prediction of the multi-cycle deformation

				Process simulation (coupled with die)				**Die stress analysis**			
	Ram speed	**Billet length**	**dwell-time**	**Temp. [C°]**		**Pressure [MPa]**		structural code (1st cycle)		Optistruct	
	[mm/s]	[mm]	[h]	Max	Min	Max	Min	$\sigma_{VM\ max}$	UZ_{max}	$\sigma_{VM\ max}$	UZ_{max}
2_legs ("A")	3	500	0.0463	588	468	391	66	1018	0.44	1809	0.43
2-legs_v25%	3.75	500	0.0370	598	473	395	68	1018	0.45	n.a.	n.a.
2-legs_AA7020	3	500	0.0463	597	473	409	61	1018	0.47	n.a.	n.a.
2-legs_1.5L	3	750	0.0695	586	467	395	68	1026	0.45	n.a.	n.a.
3_legs ("A")	3	500	0.0463	590	470	398	63	982	0.39	1479	0.33
3-legs+v25%	3.75	500	0.0370	601	475	401	66	981	0.41	n.a.	n.a.
3-legs_AA7020	3	500	0.0463	600	475	413	57	982	0.42	n.a.	n.a.
3-legs+1.5L	3	750	0.0695	586	469	400	65	995	0.40	n.a.	n.a.
4-legs ("A")	3	500	0.0463	592	471	397	52	997	0.39	1525	0.33
4-legs_v25%	3,75	500	0.0370	602	477	401	54	986	0.40	n.a.	n.a.
4-legs_AA7020	3	500	0.0463	601	477	413	49	984	0.41	n.a.	n.a.
4-legs_1.5L	3	750	0.0695	590	480	408	54	997	0.40	n.a.	n.a.

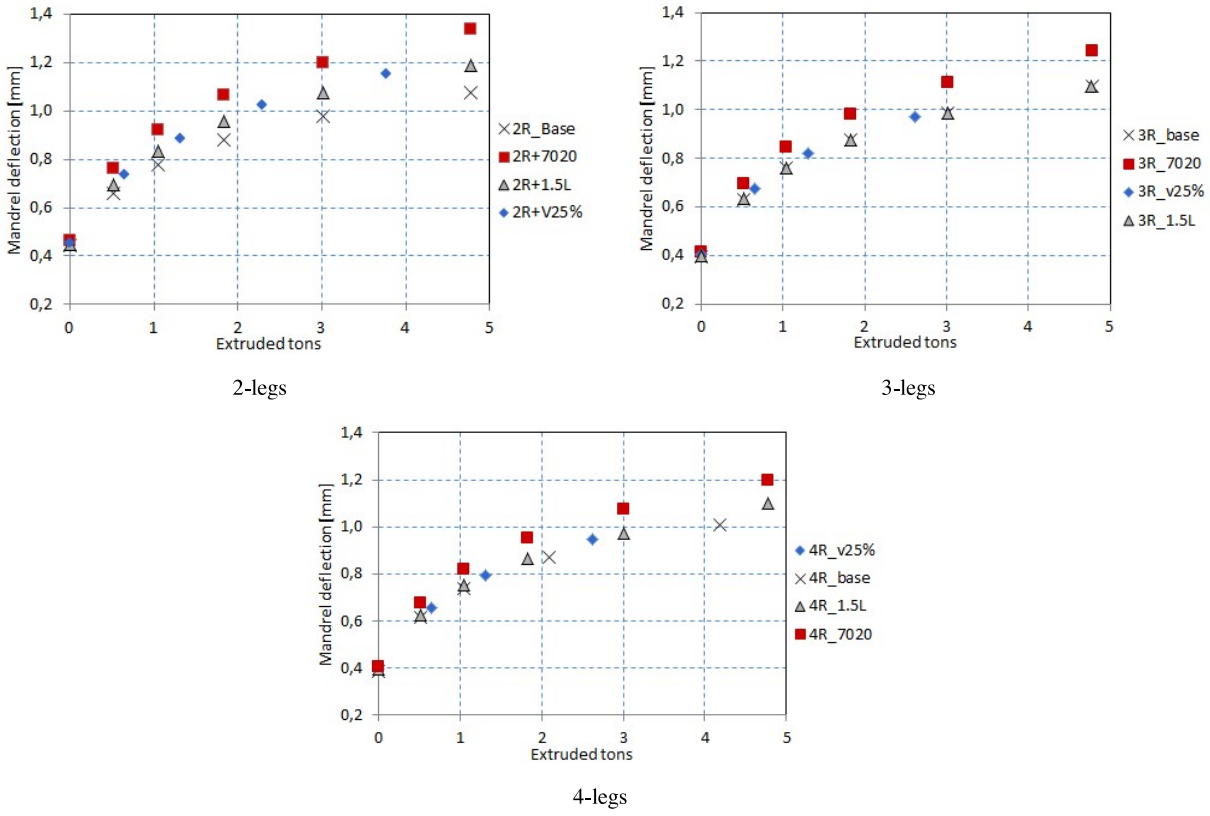

Fig.4. Prediction of the multi-cycles die deformation at the numerical DOE configurations for the three investigated configurations (2, 3, 4-legs)

5. Conclusions

As outcomes of the work, the following main observational conclusions are obtained:

- For straight ports the peak extrusion load is directly related to the total legs surface and then to the friction effect; for divergent ports the influence of friction is reduced and the peak load is inversely correlated with the ports area (higher ports involve higher deformations throughout the ports).
- A marked effect is played by a radius of 1 mm on the bearings in the reduction of both the peak extrusion load and of the pressure in the welding chamber.
- The increase in the welding chamber pressure is more sensible to the increase of the welding chamber width and less to increase of the ports dimensions.
- The 2-legs die configuration exhibits a delayed onset and a wider charge weld length if compared to the 3 and 4-legs solutions due to the higher ports volume and extended dead metal zones. If a 99% of old-new billet material replacement is considered, then a total weld length of 5,230 mm is found, 43% higher than the common industrial practice to scrap 3,000 mm if the extrusion ratio exceeds 40.
- The 2-legs die configuration exhibits the most sensible variation of die deflection to process parameters (ram speed, billet length and extruded alloy). This sensibility is progressively reduced with the increasing of the number of mandrel supporting legs. The most critical parameter affecting the die deflection is found to be the billet material; if the AA7020 is compared to the AA6005, after 5 tons of extruded material an increased die deflection of 25% is achieved for the 2-legs solution.

References

[1] Arif A.F.M., Sheikh A.K., Qamar S.Z.. A study of die failure mechanisms on aluminum extrusion, J. Mater. Proc. Tech. 124 (2003) 318-328.

[2] Donati L., Tomesani L.. The effect of die design on the production and seam weld quality of extruded aluminum profiles. J. Mater. Proc. Techn. 164-165 (2005) 1025-1031.
[3] Reggiani B., Donati L., Zhou J., Tomesani L., The role of creep and fatigue in determining the high-temperature behaviour of AISI H11 tempered steel for aluminium extrusion dies. J. Mat. Proc. Tech. 210 (2010) 1613–1623.
[4] Reggiani, L. Donati, L. Tomesani, Constitutive laws for the deformation estimation of extrusion die in the creep-fatigue regime. Key Eng. Mat. 491 (2012), 233 – 240.
[5] Velay V., Bernhart G., D., Penazzi L.. Cyclic behavior modeling of a tempered martensitic hot work tool steel. Int. J. Plasticity 22 (2006) 459–496.
[6] Liu J., Lin G., Feng D., Zou Y., Sun L. Effect of process parameters and die geometry on longitudinal welds quality in aluminum porthole die extrusion process. J. cent. South Univ. Technol. 17 (2010) 688-696.
[7] Donati L., Tomesani L., Minak G.. Characterization of seam weld quality in AA6082 extruded profiles. J. Mater. Proc. Tech. 191 (2007) 127-131.
[8] Reggiani B., Segatori A., Donati L., Tomesani L. Prediction of charge welds in hollow profiles extrusion by FEM simulations and experimental validation. Int J Adv Manuf Technol 69 (2013), 1855-1872.
[9] Mahmoodkhani Y., Wells M., Parson N., Jowett C., Poole W. Modeling the formation of transverse weld during billet-on-billet extrusion. Materials 7 (2014) 3470-3480.
[10] Donati L., Tomesani L., Schikorra M., Tekkaya A.E. Extrusion Benchmark 2007 – Benchmark Experiments: Study on Material Flow Extrusion of a Flat Die. Key Eng. Mat. 367 (2008) 1-8.
[11] Pietzka D., Khalifa N.B., Donati L., Tomesani L., Tekkaya A.E. Extrusion Benchmark 2009-Experimental analysis of deflection in extrusion dies. Key Eng. Mat. 424 (2009) 19-26.
[12] HyperXtrude (Version 12.0) Simulation Software for Extrusion Process, Altair Engineering Inc. USA. http://www. altairhyperworks.com
[13] Pinter T., Reggiani B.. Quantitative evaluation of porthole dies design practices by means of FEM analysis. In the proc. of the 8th World Congress Aluminium (2013), Milano Italy, 14-18 May 2013.
[14] Duan X., Sheppard T.. Computation of substructural strengthening by the integration of metallurgical models into the finite element code, Comput. Mater. Sci. 27 (2003) 250–258.
[15] Pinter T., El Mehtedi M., Constitutive Equations for Hot Extrusion of AA6005A, AA6063 and AA7020 Alloys. Key Eng. Mat. 491 (2012) 43-50.
[16] Donati L., Tomesani L.. The prediction of seam welds quality in aluminum extrusion. J. Mater. Proc. Tech. 153-154 (2003) 366-373.
[17] Kim K.J., Lee C.H., Yang D.Y.. Investigation into the improvement of welding strength in three-dimensional extrusion of tubes using porthole dies. J. Mater. Proc. Techn. 130-131 (2002) 426-431.